A COMPACT CIRCULAR PATCH MIMO ANTENNA WITH IMPROVED RADIATION EFFICIENCY FOR 5G MILLIMETER-WAVE APPLICATIONS

Abstract

A circular patch dual element Multiple-input-multiple-output (MIMO) antenna with an impedance bandwidth of 9.48GHz (20.83-30.31 GHz) using a partial ground plane is proposed for 5G millimeter wave applications. The envelope correlation coefficient (ECC), diversity gain (DG), mean effective gain (MEG), total active reflection coefficient (TARC), and channel capacity loss (CCL) of the MIMO antenna are addressed, and the obtained values are 0.012, 9.98dB, 3dB, -16dB, and 0.20 bits/sec/Hz, respectively. At 30GHz, the maximum gain of 8.05dBi is attained. Furthermore, a radiation efficiency of greater than 93% is attained in the frequency range of 20.83 to 30.31 GHz. The suggested MIMO antenna is built on a Rogers RO 4003 substrate with dimensions of $25\times20\times0.76mm^3$, a dielectric constant of 3.55, and a loss tangent of 0.0027.

Keywords: 5G; CCL; Millimeter wave; MIMO; Tapered fed

Authors

Ajit Kumar Singh
Department of Electronics & Communication Engineering
Indian Institute of Information Technology
Ranchi, India
ajitsingh31393@gmail.com

Santosh Kumar Mahto
Department of Electronics & Communication Engineering
Indian Institute of Information Technology
Ranchi, India
skumar@iiitranchi.ac.in

Praveen Kumar
Department of Electronics & Communication Engineering
National Institute of Technology
Jamshedpur, India 2018rsec005@nitjsr.ac.in

Rashmi Sinha
Department of Electronics& Communication Engineering
National Institute of Technology
Jamshedpur, India
rsinha.ece@nitjsr.ac.in

I. INTRODUCTION

The current wireless communication environment includes increased data speeds, higher capacity, better resolution, and reduced latency. In order to achieve the aforementioned benefit and increase the information throughput for 5G communications, the MIMO system should be employed [1], [2]. The fifth-generation (5G) mobile communication has been introduced throughout the world. For 5G technology in general, the millimeter and centimeter wave spectrum (3-300 GHz) has been chosen, which can also help with achieving the increased transmission capacity with an information rate up to a few Gbps [3], [4]. The fact that the lower frequency bands are already occupied by numerous wireless applications like Wi-Fi, WiMAX, Bluetooth, ISM, and mobile communication, etc., while the majority of the millimetre wave spectrum is still underutilized and can be used for 5G communications, is another argument in favor of choosing this spectrum [5].

Communication in this frequency range exhibits path loss, multipath fading, and neighboring channel interference [6]. While several antennas are used to lessen interference and multipath fading, high gain antennas can compensate for path loss [7]– [9]. Despite the fact that specific 5G wireless technology standards have not yet been adopted and developed, the millimeter-wave antenna is a strong competitor for streaming massive amounts of video material and offering virtual reality applications. On the other hand, many researchers have started to lay the foundation for the standard.

For 5G millimeter wave applications, a variety of MIMO antennas have been suggested in the literature [10]– [15]. A millimeter-wave dielectric resonator (DR) based MIMO antenna system was built using two linear arrays. To lessen field correlation, each array has a set beam direction that is tilted. A passive microstrip-based feed network was developed to accomplish this beam tilting [10]. A symmetrical dual-beam bowtie antenna with an optimal gain of 7 dBi was presented in [11] by combining three pairs of metamaterials (MTM) arrays. For smartphone applications, a 4G/5G MIMO antenna system was created [12]. The antenna has a measured bandwidth of 4.8 GHz and covers the spectrum from 25.7 to 30.50 GHz (18.7%). A MIMO DRA was suggested by [13] for 5G applications. The proposed antenna's simulated bandwidth spans the 28 GHz band, which is necessary for 5G applications, from 27.25 GHz to 28.59 GHz. For 5G wireless communications, a dipole array with metamaterial architecture and capacitively loaded loops was proposed. [14]. The mutual contact between the components is reduced by trimming the metamaterial region's edges. [15] Suggests an effective way to improve isolation between two tapered slot antennas. This was achieved by etching corrugations based on metamaterials.

MIMO systems are essential for increasing data rates in areas with limited bandwidth. The two most important design characteristics of a MIMO system are good isolation and low correlation. The isolation between the elements is increased by using flawed ground structures and parasitic elements between the radiating elements [16], [17]. With these approaches, it is challenging to provide a wide bandwidth while also offering low isolation and minimal correlation due to the deterioration of impedance matching. A unique millimeter-wave MIMO antenna with good element isolation is therefore needed.

This gave us the idea to design a circular microstrip 1×2 MIMO antenna with a broad frequency band and improved diversity performance. In this paper, a dual-element spatial diversity MIMO antenna with a larger impedance bandwidth and smaller size is proposed.

Section II discusses the precise structure of the design antenna. In sections III, the simulated performance of the antenna is reviewed and described. The performance of the antenna's diversity is covered in Section IV. Section V is the article's conclusion.

1. **Design:** The diagram of the circular monopole radiator, which is employed for MIMO configuration and has a dimension of 12 × 20 mm^2, shown in Fig. 1(a). The optimum dimensions for a single element in Table I are calculated using traditional antenna theory equations for circular patch antenna [18].

$$R = \frac{F}{\{1+\frac{2h}{\pi\epsilon_r F}[\ln(\frac{\pi F}{2h})+1.7726]\}^{1/2}} \quad (1)$$

Where, $$F = \frac{8.791\times10^9}{f_r\sqrt{\epsilon_r}} \quad (2)$$

Where h represents height of substrate, ε_r = dielectric constant of substrate

The fringing effect is not considered in equation (1). The effective radius (R_{eff}) of the patch is used because fringing makes the patch electrically larger, as demonstrated in equation (3).

$$R_{eff} = R\sqrt{(1+\frac{2h}{\pi.\epsilon_r a})[\ln\left(\frac{\pi R}{2h}\right)+1.7726]} \quad (3)$$

Hence, the resonant frequency for the dominant $TM^z{}_{110}$ is given by-

$$f_r = \frac{1.8412V_0}{2\pi R_{eff}\sqrt{\epsilon_r}} \quad (4)$$

Where v_0 is the speed of light in free space

Using equation (1) and (2), and the given specified data the radius of the circular patch R = 3mm. The dimensions of microstrip feed line are calculated explicitly to achieve the proper impedance matching. Figure 1 (b) represents the S11 of the monopole radiator resonating at 22.45GHz frequency with frequency band ranging from 21.08-30.53GHz.

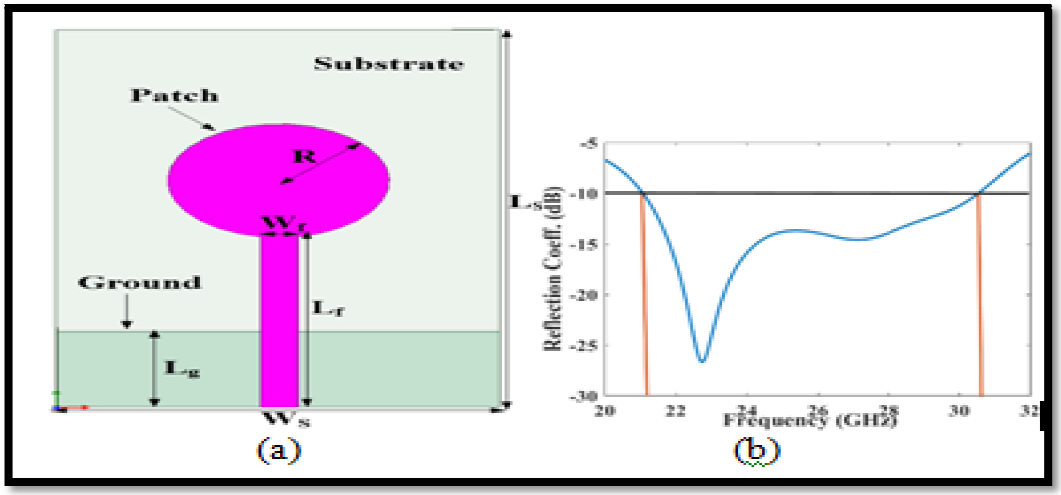

(a) (b)

Figure 1: (a) Single element (proposed) (b) Reflection coeff.

The parametric analysis of ground length L_g is been finished by varying L_g from 3mm-5mm as shown in Figure 2. The optimum matching is obtained at L_g=4mm.

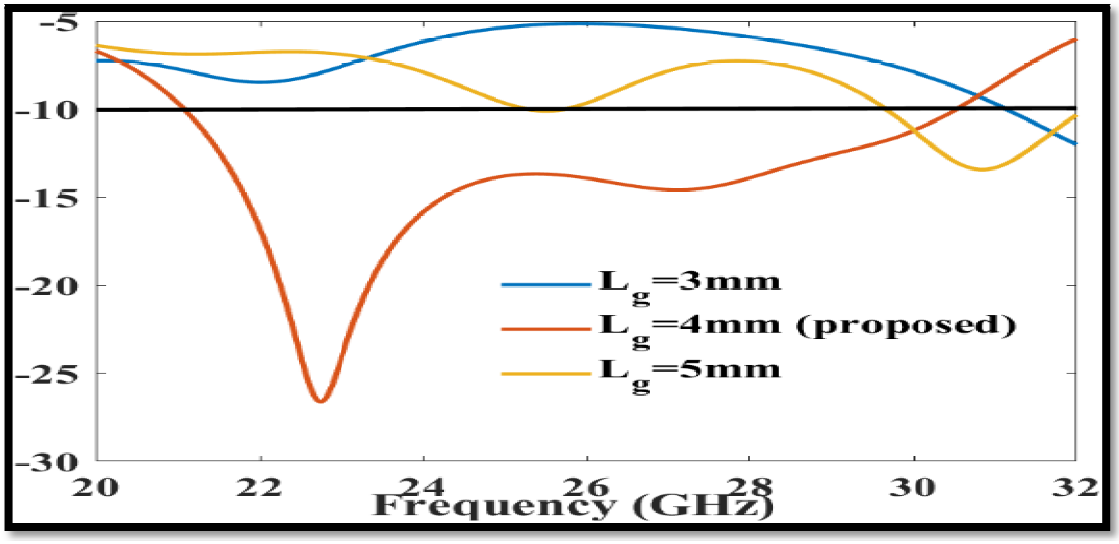

Figure 2: Parametric analysis of ground length L_g

Table 1: Dimensions of Single Element Antenna

Parameter	Value (mm)	Parameter	Value (mm)
L_S	20	W_f	1
W_S	12	R	3
L_f	9	L_g	4

A dual-port MIMO is designed as depicted in Figure. 3, by utilizing the single element antenna observed previously. The MIMO antenna occupies an area of $25\times20mm^2$, forming a rectangular shape. This design doesn't require any additional

isolation components or decoupling methods because the isolation is sufficient. The port isolation of a dual element antenna is greater than 17dB. Edge-to-edge spacing between two elements is $0.9\lambda_0$, where λ_0 is the free space wavelength at a lower frequency for a single element at 21.08GHz.

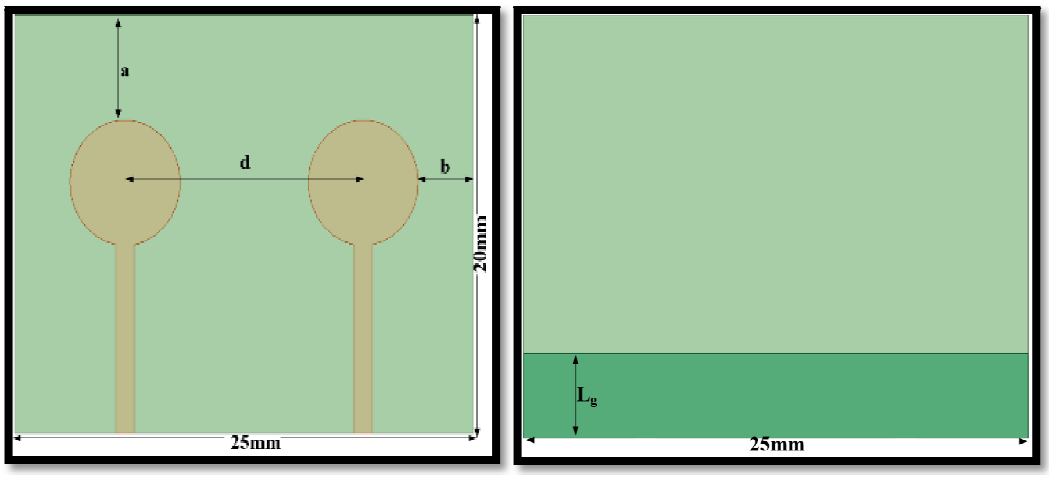

(a) (b)

Figure 3: MIMO antenna (a) Front view, (b) Back view, d=13mm ($0.9\lambda_0$), a=5mm, b=3mm

Simulated matching and isolation, as represented in Fig. 4(a) & (b) are < -10dB, -17dB respectively, throughout the entire bandwidth (20.83-30.31 GHz). The maximum return loss obtained at frequency of 28GHz is 21dB. The minimum isolation is 17dB, whereas maximum isolation up to 28.2dB.

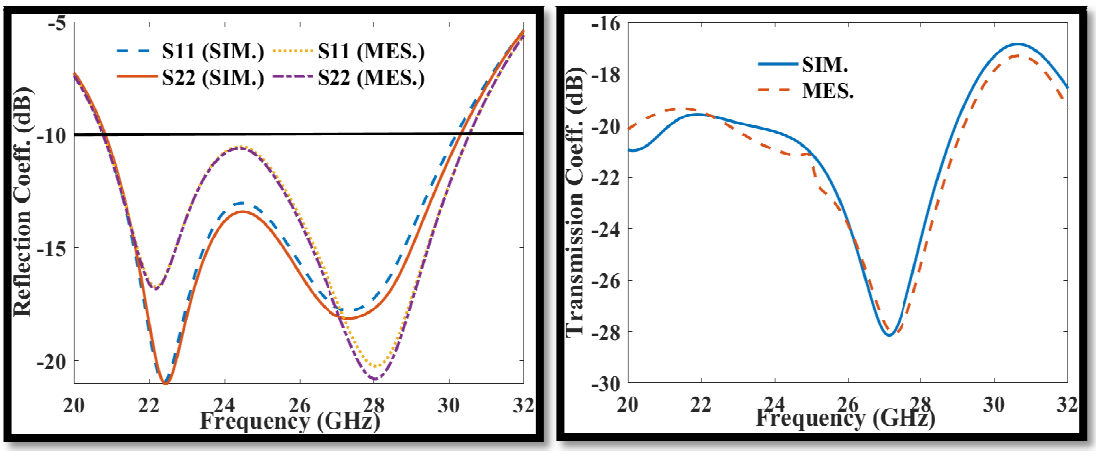

(a) (b)

Figure 4: (a) Reflection coefficient (S11) (b) Transmission coefficient (S12)

II. RESULT AND DISCUSSION

The antenna's peak gain is depicted in Figure 5(a). The antenna's peak gain ranges from 7.12dBi to 8.05dBi. Fig. 5(b) shows the proposed antenna's radiation efficiency. Throughout the whole bandwidth (20.83-30.31 GHz), the radiation efficiency ranges from 97.1% to 98.2%. Fig. 6 represents the Co and Cross polarization of proposed antenna at 22.5GHz and 28GHz frequencies at x-z and y-z plane respectively. Furthermore, because the estimated axial ratio is greater than 15 dB, the suggested antenna is linearly polarized. In comparison to the co polar pattern, the cross polar pattern is smaller. Fig. 7 depicts the distribution of the surface current of a dual element MIMO antenna operating at 22.5GHz. Surface currents flow from stimulated port-1 to port-2 in Figure. 7are the primary cause of isolation between neighboring antenna elements. Because of the excitation of one port and the termination of another port with matched load, other ports have a low surface current. The fabricated MIMO antenna is shown in Figure. 8

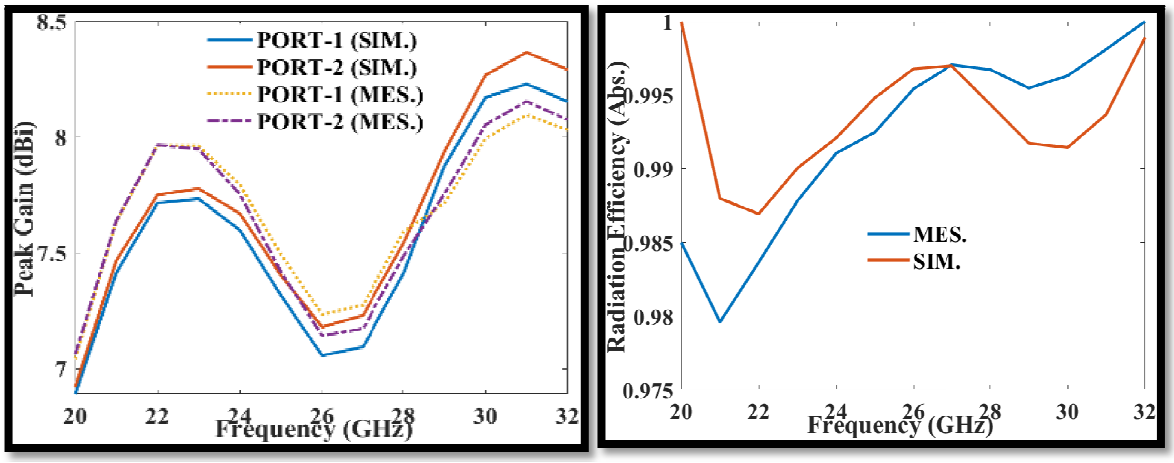

(a) (b)

Figure 5: (a) Peak Gain (b) Radiation Efficiency

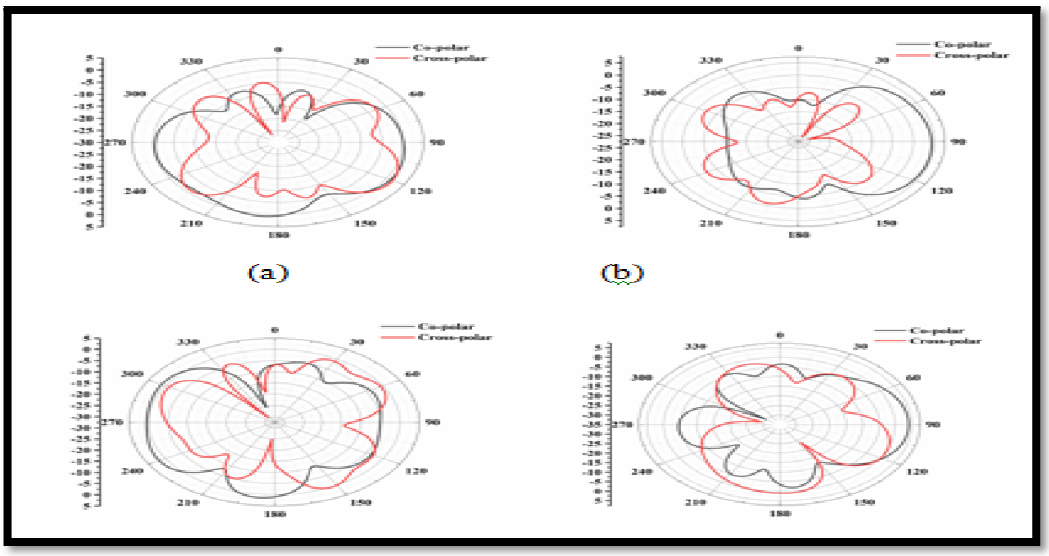

Figure 6: Co & Cross (a) YZ plane at 22.5GHz (b) ZX plane at 22.5GHz (c) YZ plane at 28GHz (d) ZX plane at 28GHz

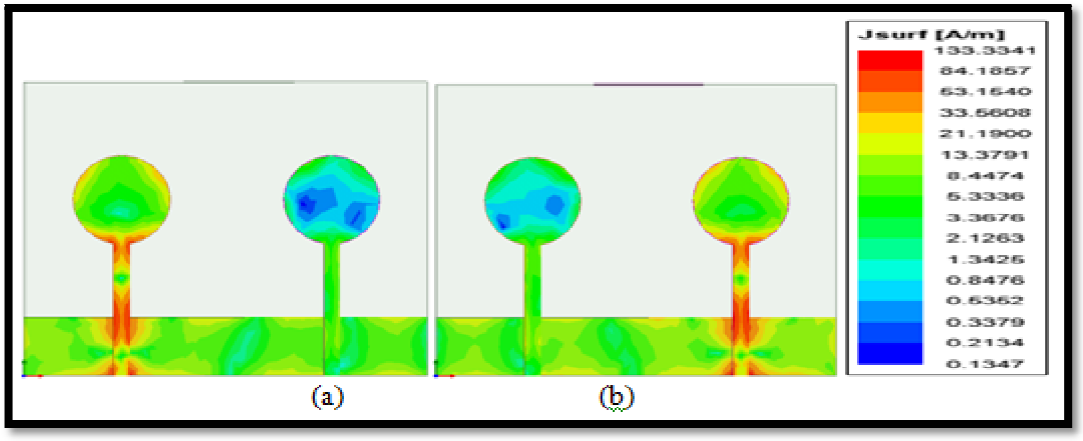

Figure 7: Surface current density (a) PORT-1 (b) PORT-2

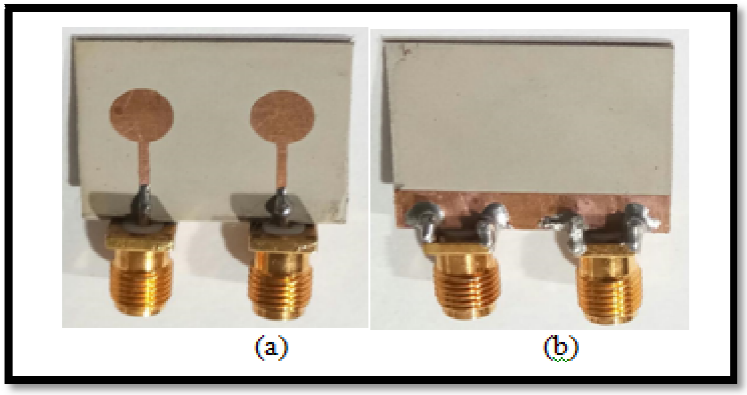

Figure 8: Fabricated MIMO antenna (a) Front view (b) Back View

III. MIMO DIVERSITY PERFORMANCE

The ECC, DG, TARC, CCL, and MEG are crucial MIMO diversity and multiplexing factors that assure the suggested structure's operation. The ECC which considers radiation pattern, polarization, and relative phase of the fields can be calculated using (5) [19],

$$ECC = \frac{\left|\iint_{4\pi} F_1^*(\theta,\varphi).F_2(\theta,\varphi)d\Omega\right|^2}{\iint_{4\pi}|F_1(\theta,\varphi)|^2 \times \iint_{4\pi}|F_2(\theta,\varphi)|^2 d\Omega} \quad (5)$$

The MIMO antenna's DG is determined as follows: -

$$DG = 10\sqrt{1 - ECC^2} \quad (6)$$

DG should be near to 10dB. As displayed in Fig. 9(a) and (b), the computed ECC and DG are < 0.012 and 9.98dB, respectively, indicating good diversity performance.
TARC is a crucial metric in dual-port antennas since it shows the relationship between radiated and received power. The TARC of the two-port antenna can be determined as follows:

$$TARC = \frac{\sqrt{(S_{11}+S_{12})^2+(S_{21}+S_{22})^2}}{\sqrt{4}} \quad (7)$$

For MIMO systems, TARC should ideally be < 0dB. The TARC has a simulated value of < -6dB, as shown in Fig.9(c). MEG is a metric for calculating the median power from the event power [20]. For two element MEG can be determined using equation (8) and (9) and shown in Fig.9(d),

$$MEG_i = 0.5\left[1 - \sum_{j=1}^{N} |S_{ij}|^2\right] < -3dB \quad (8)$$

$$MEG_j = 0.5\left[1 - \sum_{i=1}^{N} |S_{ij}|^2\right] < -3dB \quad (9)$$

$$\left|MEG_i - MEG_j\right| < 3dB \quad (10)$$

$$\left|\frac{MEG_i}{MEG_j}\right| = \pm 3dB \quad (11)$$

i and j, respectively, stand for the first and second antenna elements. CCL is calculated using equation (12) [21] for dual-element MIMO antenna, as represented in Fig.9(e). Practically, CCL operates at less than 0.4 bits/second/Hz.

$$CCL = -\log_2 det[\beta^R] \quad (12)$$

$$[\beta^R] = \begin{bmatrix} \beta_{ii} & \beta_{ij} \\ \beta_{ji} & \beta_{jj} \end{bmatrix}$$

$$\beta_{ii} = 1 - \left(\sum_{j=1}^{N} |S_{ij}|^2\right)$$

$$\beta_{ij} = -\left(S_{ii}^* S_{ij} + S_{ji}^* S_{ij}\right)$$

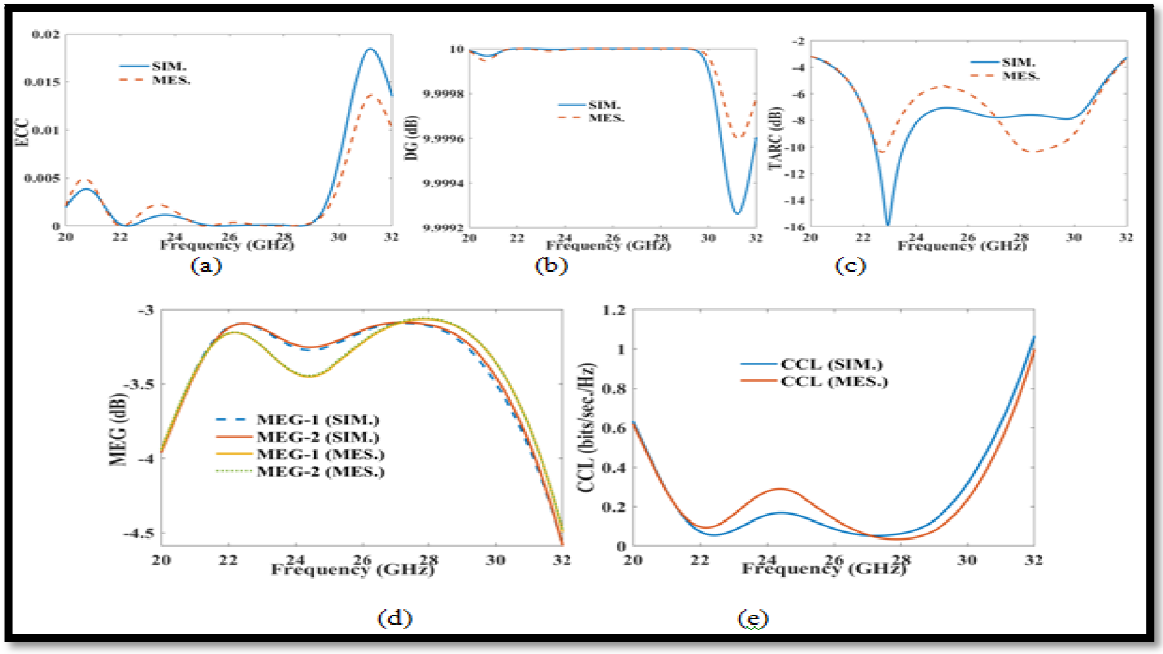

Figure 9: (a) ECC (b) DG (c) TARC (d) MEG (e) CCL

Table 2: Comparative Table of Proposed mm-wave MIMO Antenna

Ref.	**Frequency band (GHz)**	**Size (mm^2)**	**Isolation(dB)**	**ECC**	**Avg. Gain (dBi)**
[10]	29.75-31.50	1008	25	0.002	8.13
[11]	24.25-27.5	915	NA	NA	7.03
[12]	25.7-30.5	5625	15	0.16	8.73
[13]	27.25-28.59	400	24	0.013	8072
[14]	26-31	1488	21	0.015	9.06
[15]	27-32	3570	37.1	NA	17.9
[P]	**20.83-30.31**	**500**	**20**	**0.012**	**8.05**

Table 2 compares the proposed MIMO antenna to prior published studies. Except for [13], the MIMO antenna is 500mm^2 in size, which is quite small. The MIMO antenna attained a 9.48GHz impedance bandwidth and a total efficiency of 90%, which is good, however ECC less than [10]. As a result, the proposed antenna has a number of advantages, including planar geometry, wide bandwidth, and low mutual coupling, which are important for 5G MIMO system

IV. CONCLUSION

A circular shaped dual-element MIMO antenna for millimeter-wave applications with a minimum isolation of 17dB is proposed. Performance of the suggested design was assessed and discussed in terms of a number of antenna metrics, including impedance bandwidth, gain, efficiency, and diversity characteristics. The proposed design is fabricated and measured, and

found a good agreement between simulated and measured result. As a result, the MIMO antenna developed is a viable choice for millimeter-wave applications.

REFERENCES

[1] Z. Pi and F. Khan, "An introduction to millimeter-wave mobile broadband systems," IEEE communications magazine, vol. 49, no. 6, pp. 101– 107, 2011.
[2] Z. Ren and A. Zhao, "Dual-band mimo antenna with compact self-decoupled antenna pairs for 5g mobile applications," IEEE Access, vol. 7, pp. 82288–82296, 2019.
[3] Z. H. Abbas, M. S. Haroon, G. Abbas, and F. Muhammad, "Sir analysis for non-uniform hetnets with joint decoupled association and interference management," Computer Communications, vol. 155, pp. 48– 57, 2020.
[4] M. S. Haroon, Z. H. Abbas, F. Muhammad, and G. Abbas, "Coverage analysis of cell-edge users in heterogeneous wireless networks using stienen's model and rfa scheme," International Journal of Communication Systems, vol. 33, no. 10, p. e4147, 2020.
[5] J. Khan, D. A. Sehrai, M. A. Khan, H. A. Khan, S. Ahmad, A. Ali, A. Arif, A. A. Memon, and S. Khan, "Design and performance comparison of rotated y-shaped antenna using different metamaterial surfaces for 5g mobile devices," Comput. Mater. Contin, vol. 2, pp. 409–420, 2019.
[6] L. Swindlehurst, E. Ayanoglu, P. Heydari, and F. Capolino, "Millimeter-wave massive mimo: The next wireless revolution?" IEEE Communications Magazine, vol. 52, no. 9, pp. 56–62, 2014.
[7] H. Jin, W. Che, K.-S. Chin, G. Shen, W. Yang, and Q. Xue, "60-ghz ltcc differential-fed patch antenna array with high gain by using soft-surface structures," IEEE Transactions on Antennas and Propagation, vol. 65, no. 1, pp. 206–216, 2016.
[8] O. Yurduseven and D. R. Smith, "Dual-polarization printed holographic multibeam metasurface antenna," IEEE Antennas and Wireless Propagation Letters, vol. 16, pp. 2738–2741, 2017.
[9] X. Cheng, Y. Yao, T. Tomura, J. Hirokawa, T. Yu, J. Yu, and X. Chen, "A compact multi-beam end-fire circularly polarized septum antenna array for millimeter-wave applications," IEEE Access, vol. 6, pp. 62784– 62792, 2018.
[10] M. S. Sharawi, S. K. Podilchak, M. T. Hussain, and Y. M. Antar, "Dielectric resonator based mimo antenna system enabling millimeter wave mobile devices," IET Microwaves, Antennas & Propagation, vol. 11, no. 2, pp. 287–293, 2017.
[11] H. Jiang, L.-M. Si, W. Hu, and X. Lv, "A symmetrical dual-beam bowtie antenna with gain enhancement using metamaterial for 5g mimo applications," IEEE Photonics Journal, vol. 11, no. 1, pp. 1–9, 2019.
[12] M. Ikram, M. Sharawi, A. Shamim, and A. Sebak, "A multiband dualstandard mimo antenna system based on monopoles (4g) and connected slots (5g) for future smart phones," Microwave and Optical Technology Letters, vol. 60, no. 6, pp. 1468–1476, 2018.
[13] Y. Zhang, J.-Y. Deng, M.-J. Li, D. Sun, and L.-X. Guo, "A mimo dielectric resonator antenna with improved isolation for 5g mm-wave applications," IEEE Antennas and Wireless Propagation Letters, vol. 18, no. 4, pp. 747–751, 2019.
[14] Z. Wani, M. P. Abegaonkar, and S. K. Koul, "A 28-ghz antenna for 5g mimo applications," Progress In Electromagnetics Research Letters, vol. 78, pp. 73–79, 2018.
[15] S. Gupta, Z. Briqech, A. R. Sebak, and T. A. Denidni, "Mutual-coupling reduction using metasurface corrugations for 28 ghz mimo applications," IEEE Antennas and Wireless Propagation Letters, vol. 16, pp. 2763– 2766, 2017.
[16] M. S. Sharawi, "Current misuses and future prospects for printed multiple-input, multiple-output antenna systems [wireless corner]," IEEE Antennas and Propagation Magazine, vol. 59, no. 2, pp. 162–170, 2017.
[17] S. Painam, V. S. Anumala, K. Painam, K. C. Tatikonda, S. Miriyala, and P. Prasad, "Triple-uwb millimeter-wave mimo antenna with improved isolation for 5g wireless applications," in 2019 IEEE Indian Conference on Antennas and Propogation (InCAP), pp. 1–5, IEEE, 2019.

[18] A. Balanis, Antenna theory: analysis and design. John wiley & sons, 2015.
[19] K. Singh, S. K. Mahto, P. Kumar, R. K. Mistri, and R. Sinha, "Reconfigurable circular patch MIMO antenna for 5G (sub-6 GHz) and WLAN applications," International journal of communication system, e5313, 2022.
[20] A. Glazunov, A. F. Molisch, and F. Tufvesson, "Mean effective gain of antennas in a wireless channel," IET microwaves, antennas & propagation, vol. 3, no. 2, pp. 214–227, 2009.
[21] K. Singh, S. K. Mahto, and R. Sinha, "A miniaturized mimo antenna for c, x, and ku band applications," Progress In Electromagnetics Research C, vol. 117, pp. 31–40, 2021

